Chapter 8

Effects of Post Treatments on Bismuth-Doped and Bismuth/Erbium Co-doped Optical Fibres

Shuen Wei, Mingjie Ding, Desheng Fan,
Yanhua Luo, Jianxiang Wen and Gang-Ding Peng

Additional information is available at the end of the chapter

http://dx.doi.org/10.5772/intechopen.75106

Abstract

Bismuth-doped and bismuth/erbium co-doped optical fibres have attracted much attention for their great potential in the photonic applications at ultrawide O, E, S, C and L bands. The effects of post treatments, including various heating, high energy ray radiation, laser radiation and H_2 loading processes, on these fibres' performance, functionality and stability have been experimentally studied. Experimental results demonstrate that these post treatments could allow us to get insights regarding the formation and the structure of bismuth active centre (BAC) and be used to control and regulate the formation of BAC.

Keywords: bismuth-doped fibre (BDF), bismuth and erbium co-doped optical fibre (BEDF), bismuth active centre (BAC), broadband, post treatments, thermal treatment, gamma radiation, photo-bleaching, H_2 loading

1. Introduction

Since the first demonstration of the broadband near infrared (NIR) luminescence in the bismuth-doped silicate glass [1], bismuth-doped materials, including crystal, glass, fibre, and so on, have been developed and studied for photonic applications at the extended band [2–7]. Especially, bismuth-doped optical fibres (BDFs) have been developed for fibre amplifiers and lasers from 1250 to 1500nm and 1600 to 1800nm [8–13]. Later on, Bi/Er co-doped silicate optical fibres (BEDFs), due to their great potential in photonic applications from 1150 to 1700nm covering both the used bandwidth (C band) and the huge unused bandwidth, have been proposed and developed [14–16].

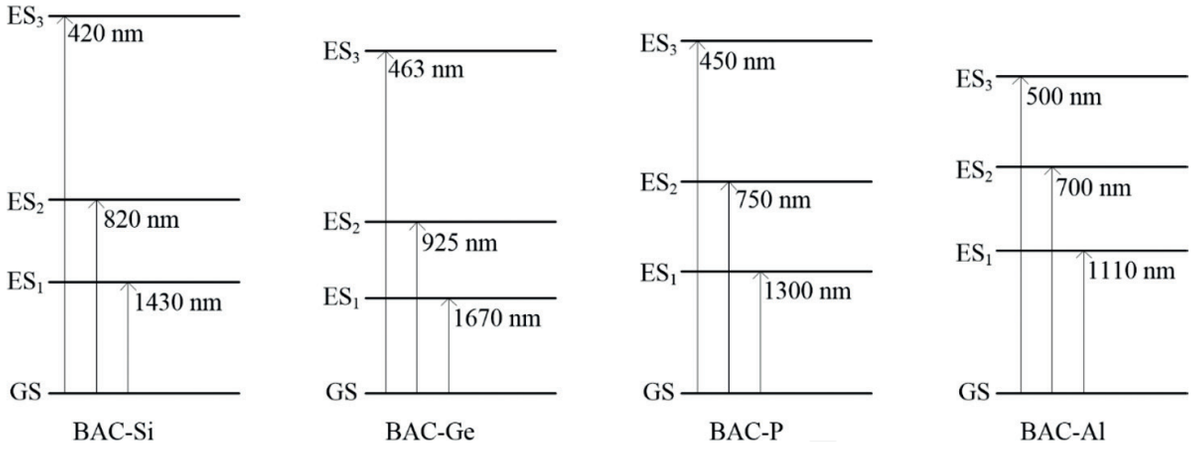

Figure 1. Energy level diagrams of different BACs in BDFs.

Although there have been a lot of breakthroughs in the unused spectral range, there remain many prominent scientific and technological challenges [17, 18]. The fundamental understanding of NIR emitting BAC is one key challenge. Unlike the well-shielded *f-f* transitions of Er^{3+}, the electronic transition of the unshielded Bi centre(s) is closely linked to the microenvironment. According to the type of the local environment, there are four types of BACs in BDFs, which are BAC-Si, BAC-Ge, BAC-P and BAC-Al, linked to SiO_2, GeO_2, P_2O_5:SiO_2 and Al_2O_3:SiO_2, respectively [18]. Their energy diagrams are shown in **Figure 1**.

Previous reports have demonstrated that the formation of BAC greatly depends upon the processing conditions. More specifically, BAC can be activated by high-intensity femtosecond laser [19], high-temperature melting [20, 21], γ-radiation [22, 23], and so on. Here, effects of post treatments on BDF and BEDF by thermal treatment, high energy ray radiation, laser radiation and H_2 loading have briefly been reviewed. It is generally believed that these post treatments will greatly change the spectroscopic properties of these fibres via the variation of the BAC. Further research into reasons of variations will help to understand BAC. With further understanding of the BAC, it is also hopeful to find an appropriate way to control and regulate the BAC for the performance improvement of BDF and BEDF.

2. Thermal treatment

It is known that the unshielded outer electron shell of bismuth makes the energy structure of Bi more complex and closely related to the microstructure of the host material [18]. In addition, Bi itself, as a polyvalent element, often undergoes oxidation-reduction (redox) reaction in molten glass, which is significantly influenced by the melting temperature, atmosphere and composition [12, 20, 21, 24–26]. In general, this redox reaction moves toward the reduction side with increasing melting temperature, and the variation of the valence state of Bi can be represented as follows [12, 24]:

$$Bi^{3+} \rightarrow Bi^{2+} \rightarrow Bi^{+} \rightarrow Bi \rightarrow \text{Bi clusters}\left(\text{e.g., } Bi_2,\ Bi_2^{-},\ Bi_3\right) \rightarrow (Bi)_n \text{ colloids} \qquad (1)$$

These facts make it difficult to determine the exact nature of BACs in BDF and BEDF as the redox reaction mentioned above often occurs during the preform fabrication and fibre drawing processes. In spite of that, the reduction processes have hinted that BACs most likely consist of Bi with low valence state [27], although it is still controversial. The latest experimental data has already confirmed that BACs are the clusters consisting of Bi ions and oxygen deficiency centres instead of Bi ions themselves [12].

Since valence states of Bi as well as the deficiency [28] can be altered at high temperature, post thermal treatment has become a common method to modify the properties of Bi-doped glasses/fibres, and thus to further investigate the origin of BACs [25, 29]. Therefore, in this section, the effects of the thermal treatment upon BDFs and BEDFs, summarized and listed in **Table 1**, are presented and discussed.

2.1. Bismuth-doped fibres

2.1.1. BAC emission at high temperature

In terms of BDFs, the emission of BACs at high temperature of aluminosilicate fibres have been reported as early as 2008 [30]. However, their interpretations are not convincible owing to the limited data. Later on, thermal effects on emission of BAC-Si at 830 nm and 1420 nm under 808 nm pumping have been studied in bismuth-doped silicate fibres (SBi) [31, 32], bismuth-doped germanosilicate fibre (GSBi) [31] as well as bismuth-doped silicate tube (SBi*) [33] (**Table 1**). It is observed that the emission of BAC-Si at ~1420 nm shows an increasing trend when treating at a specific high temperature, along with the reduction of emission at 830 nm. It is believed that the increase of NIR emission is associated with the increase of the non-radiative transition rate between ES_2 and ES_1 of BAC-Si (**Figure 1**) at high temperature, which is confirmed by the lifetime results in GSBi [31] and SBi* [33]. Taking GSBi [31] for example, the lifetime at ES_2 of BAC-Si drops directly from 30 μs to <3 μs, whereas the lifetime of 1400nm luminescence decreases by 25% when heating from room temperature to 900°C, as shown in **Figure 2**.

2.1.2. Formation of BACs

The preform of SBiO (**Table 1**) shows luminescence and absorption in both visible and NIR region before drawing, whereas SBiO drawn with oxygen in holes has no luminescence but low background loss. However, when SBiO listed in **Table 1** is annealed with argon in holes at 1100°C for 30 minutes, absorption bands of BAC-Si at 830 nm and 1420 nm appear, accompanied by the increment of the background loss [29]. The appearance of absorption at 830 and 1420 nm indicates the formation of BAC-Si, which is further confirmed by the observation of luminescence after annealing [29]. On the contrary, when SBiO is annealed with oxygen in holes, no obvious change can be detected [29]. These results demonstrate that Bi ions in BAC-Si can be oxidized into the high valence state in an oxidizing atmosphere, resulting in the decrease of both luminescence and background loss, vice versa, annealing bismuth-doped silicate glasses in argon can lead to the high background loss and possible formation of BAC-Si. These facts indicate not only the formation of BAC-Si, but also the association of BAC-Si with the low valence state of bismuth ions.

Fibre	Fabrication techniques	Core composition	λ_{ex} (nm)	λ_{em} (nm)	FWHM (nm)@ λ_{em} (nm)	Lifetime (μs)@ λ_{em} (nm)	Treatment conditions	Reference
Emission at high temperature								
SBi-P	PIT	100SiO_2-Bi(<0.02 at%)	808	830; 1400	72@1400	—	23–700°C in air	[31]
SBi* (quartz glass)	SPCVD	100SiO_2-Bi(<10^{19} cm^{-3})		825; 1420	14@825; 120@1420	60@825; 658@1420	23–600 °C in air	[33]
SBi	SPCVD	100SiO_2-Bi(<0.02 at%)		830; 1420	30@830; 117@1420	—	23–600 °C in air	[32]
SBi-LF	SPCVD	100SiO_2-Bi(<0.02 at%)-low flourine doping in core			36@830; 117@1420	—	23–500°C in air	
SBi-HF	SPCVD	100SiO_2-Bi(<0.02 at%)-high flourine doping in core			36@830; 107@1420	—	23–500°C in air	
SBi-H (holey fibre)	FCVD	100SiO_2-Bi(<0.02 at%)		830; 1400	87@1400	—	23–500°C in air	[31]
GSBi	MCVD	95SiO_2–5GeO_2-Bi(<0.02 at%)			94@1400	600@1400	23–400°C in air	
Thermal annealing								
SBiO (holey fibre)	FCVD	100SiO_2–Bi_2O_3(~0.03 at%)	337; 454-676; 975; 1064	Absence	—	—	1100°C in argon 1100°C in oxygen	[29]
ASBiY	MCVD	SiO_2-Al_2O_3-P_2O_5-Y_2O_3	750	1120	177@1120	10@820; 800@1150	≥550°C in air	[34]
ASBi	MCVD	SiO_2-Al_2O_3-Bi_2O_3	532	700; 1100	136@700; 171@1100	—	1200°C in air	[35]
SBi-H (holey fibre)	FCVD	100SiO_2-Bi(<0.02 at%)	808	830; 1400	87@1400	—	1200°C in air	[31]
GSBi	MCVD	95SiO_2–5GeO_2–Bi_2O_3(<0.02 at%)			94@1400	30@830; 600@1400	>400°C in air	
SBi-HF	SPCVD	100SiO_2-Bi(<0.02 at%)-high flourine doping in core			87@1400	—	600 °C in air	[32]
BEDF	MCVD	SiO_2-Al_2O_3-GeO_2-P_2O_5-Er_2O_3-Bi_2O_3	830	1420	98@1420	—	800°C in air 100°C/200°C/ in air	[36] [37]

Note: PIT—powder in tube, SPCVD—surface plasma chemical vapour deposition, FCVD—furnace chemical vapour deposition, MCVD—modified chemical vapour deposition.

Table 1. Summary of designations, fabrication techniques, core compositions, the excitation and emission peak wavelengths, full-width at half maximum (FWHM) of luminescence bands, and lifetime of Bi luminescence and thermal treatment conditions of BDFs.

http://dx.doi.org/10.5772/intechopen.75106

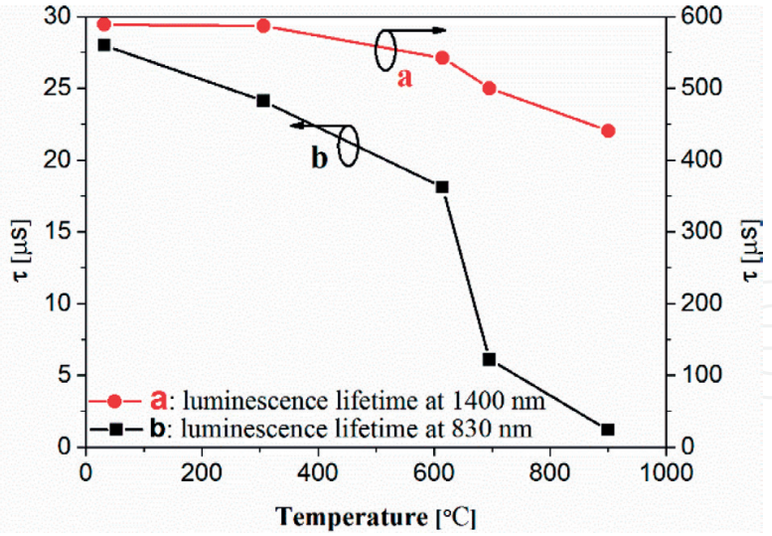

Figure 2. Luminescence lifetime at the wavelength of 830 and 1400 nm as a function of temperature excited at 808 nm [31].

Similar effects have been observed when ASBiY [34] is annealed at ≥550°C and ASBi at 1200°C [35] as listed in **Table 1**. After annealing, absorption peaks of BAC-Al at 500, 750 and 1000 nm increase, and the NIR emission at 1150 nm is enhanced. These changes obviously indicate the formation of BAC-Al. Hence, it is believed that the extra "generation" (formation of BAC-Si or BAC-Al) is associated with the reduction of $Bi^{3+} \rightarrow Bi^{2+} \rightarrow Bi^{+} \rightarrow Bi^{0}$ at high temperature [34].

2.1.3. Degradation of BACs

However, in some cases, luminescence at 1420 nm of BAC-Si starts to decrease when fibre is annealed at the high temperature in air. Such phenomenon is very prominent in BEDF [37], fabricated by conventional MCVD combined with in situ solution doping technique. When one BEDF is annealed at each prescribed temperature for 1 hour and slowly cooled down to the room temperature, without significant variation of background loss, the luminescence

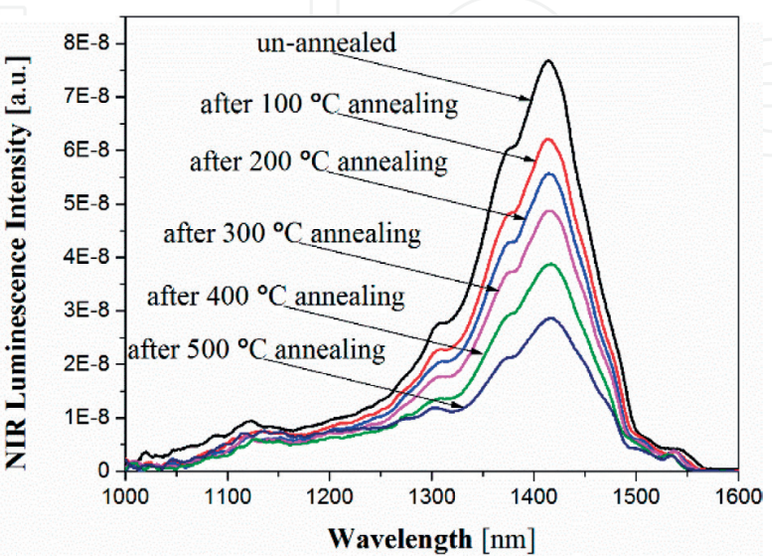

Figure 3. NIR emission spectra of BEDF after annealing at different temperatures under 830 nm excitation [37].

at 1420 nm excited at 830 nm starts to decrease after 100°C annealing, as shown in **Figure 3**, showing the degradation of BAC-Si. The degradation is attributed to the redistribution of point defect in annealed BEDF [37].

In addition, the reduction of emission of BAC-Si has also been observed in SBi-H, SBi-HF and GSBi after annealing at high temperature, as listed in **Table 1** [31, 32]. The features, behaviours and causes of these phenomena vary case by case. In SBi-H, the dissociation of BAC-Si is due to the oxygen diffusion (oxygen with high temperature tends to form an oxidation atmosphere). Another possibility is the reconfiguration of clusters in a greater porosity in SBi-HF [32], resulting in an irreversible reduction of their luminescence. In addition, the dissociation of BAC-Si due to the oxidation by GeO_2 is also observed in GSBi [31], although it is a reversible process.

2.1.4. Thermal darkening

A strong and irreversible thermal darkening effect has also been found in both BEDF and SBiO annealed at high temperature as listed in **Table 1**. When a section of BEDF is heated from room temperature to 800°C and slowly cooled down, the background losses irreversibly increase in both visible and NIR regions, which make NIR luminescence almost undetectable after annealing. Such darkening effect is obvious when comparing the radial profile of visible light intensity in the unannealed and 800°C annealed BEDF from an optical microscope, as shown in **Figure 4**.

A similar increase in background loss is observed in the annealed SBiO, of which the background loss starts to increase significantly from 600°C and up [29]. Such growths of the background loss observed in both BEDF and SBiO are consistent with Mie theory's hyperbolic dependence: $(A/\lambda) + B$, where A is assumed to be mainly determined by the average value of the product of the concentration and the volume of particles at different temperatures, B is correction constant, and λ is the wavelength of incident light. So the increment of the background loss is attributed to the formation of the metallic bismuth nanoparticles $(Bi)_n$ [29, 36, 38, 39].

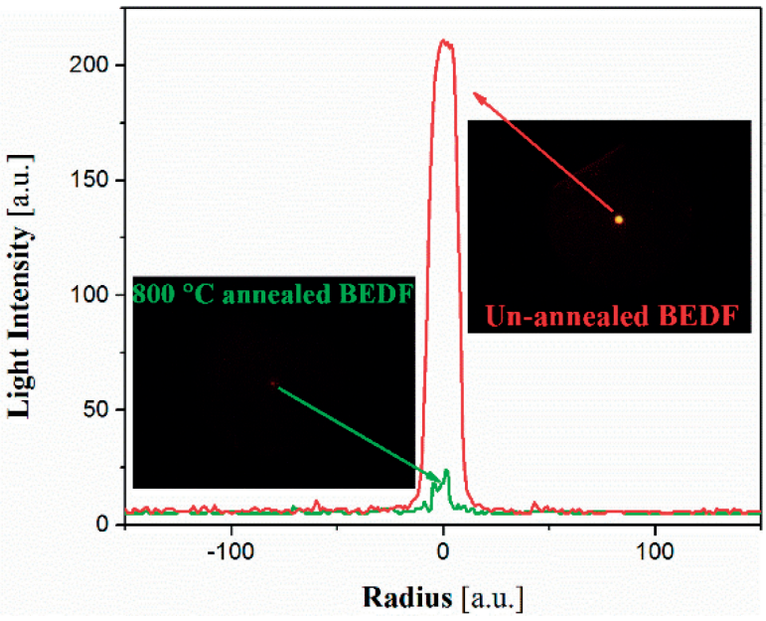

Figure 4. Radial profile of visible light intensity in the un-annealed and 800°C annealed BEDF (~2 cm) [36].

The origin of the growth of background loss is further linked to the excessive reduction of bismuth ions in Bi-doped silicate fibres [29, 36].

3. High energy ray treatment

Radiation technologies with high-energy rays, already established in materials processing, have properties uniquely suited for the creation of new advanced materials. When fibres are exposed to radiation, a darkening process occurs due to the formation of colour centres (or defects), in which radiation-induced-absorption (RIA) is observed. Extensive studies on radiation-induced darkening on pure silica and rare-earth-doped fibres have been carried out for assessing the radiation effects on fibres and understanding the possible underlying mechanisms as well as the possible use in space-borne applications [40–46].

For BDFs, radiation by high-energy rays has resulted in variations (decrease or increase) of the characteristic absorption and luminescence of corresponding BACs, thus further providing information on their properties. Moreover, it has been reported that gamma-ray irradiation can increase the density of BAC leading to an enhancement of fluorescence [47, 48]. The activation of BAC by radiation is ascribed to the reduction of Bi^{3+} to low valence state, which contributes to the NIR fluorescence by capturing radiation-released free electrons [23].

3.1. Gamma-radiation effect

Gamma radiation seems to favour the formation of new BACs in BDF, BEDF and Bi/Er/Yb co-doped fibres (BEYDFs). Wen et al. observe the radiation-induced increase of Bi ion absorption peaks as well as enhancement of photoluminescence in BDF fabricated by MCVD and atomic layer deposition technique [47]. Apart from the radiation-induced increase of Bi ion absorption, a new peak at ~580 nm arises, increasing with the increment of the dosage, which is related to the formation of aluminium oxygen hole centres (Al-OHCs). This radiation-induced defect, together with radiation-induced background increase, causes a slight decrease of NIR fluorescence excited at 532 nm. However, when pumped by 980 nm excitation, the fibres exhibit an enhancement of emission at 1410 nm of BAC-Si and at 1150 nm of BAC-Al. Besides that, their result also indicates that BAC-Al is less sensitive to radiation than BAC-Si. The enhanced fluorescence may originate from the valence state conversion as follows:

$$Bi^{5+} + 2e \xrightarrow{h\upsilon} Bi^{3+} \tag{2}$$

$$Bi^{5+} + 4e \xrightarrow{h\upsilon} Bi^{+} \tag{3}$$

$$Bi^{5+} + 5e \xrightarrow{h\upsilon} Bi^{0} \tag{4}$$

$$Bi^{3+} + 2e \xrightarrow{h\upsilon} Bi^{+} \tag{5}$$

$$Bi^{3+} + 3e \xrightarrow{h\upsilon} Bi^{0} \tag{6}$$

With the γ irradiation of BEDF from 1.0 to 50 kGy, the absorption at 830 nm is increased significantly while the absorption at a longer wavelength is reduced and emission is restrained [48–50]. The results show that BAC can be activated by gamma irradiation. A comparative study of gamma radiation effect upon BEDF and BEYDF indicates that Yb co-doping to BEDF will enhance the activation of BAC. The enhancement might be due to Compton electron capture of Yb^{3+}: $Yb^{3+} + e^{-} \rightarrow Yb^{2+}$ [42], confirmed by the reduction of the Yb^{3+} characteristic absorption at ~980 nm [48]. Moreover, the report by Sporea et al. has suggested that gamma irradiation can be used for tailoring the luminescence properties of BEDF [50]. Investigation on RIA of irradiated BEDF also suggests that BEDFs have good radiation resistance to low and moderate gamma irradiation.

Gamma-radiation effect on bismuth-doped germanosilicate fibres has recently been reported by Firstov et al. through measurement of absorption and emission after post irradiation annealing [51]. A series of BDFs with various bismuth and GeO_2 are subjected to ^{60}Co-source to different total doses of 1–8 kGy. No significant changes in the absorption and emission bands of BACs by gamma irradiation are observed. From the RIA analysis, it demonstrates that RIA is dependent upon fibre composition, where higher germanium and bismuth concentrations lead to higher radiation sensitivity.

3.2. Electron-radiation effect

Besides of gamma radiation, electron irradiation is another alternative method to change the valence state of Bi, similar to that of gamma irradiation in Bi: α-BaB_2O_4 single crystal [23]. Kir'yanov et al. studied the effect of electron irradiation in bismuth-doped germane- and alumina-silicate fibres and observed two opposite effects (decrement/increment) [52, 53]. Both fibres fabricated by MCVD and solution-doping methods are exposed to electrons of high energy (6 MeV) at room temperature to different total doses of 2×10^{12}, 1×10^{13} and 5×10^{13} cm^{-2}, respectively. Different from general behaviour of background loss increase with increasing doses, the resonant absorption peaks of Bi centres decrease with higher radiation doses, indicating a radiation-induced bleaching effect for Bi centres by electron irradiation. Deeper comparative study on fluorescence spectra of pristine and irradiated fibres reveals that the fluorescence emission spectra and lifetimes are slightly influenced by electron irradiation and the absorption changes are ascribed to the concentration change of Bi centres. Different from bismuth-doped germane-silicate optical fibre, bismuth-doped alumina-silicate fibre exhibits an increase of BAC-Al due to the electron irradiation.

4. Laser radiation

Femtosecond laser irradiation at 800 nm is reported to facilitate the activation of emission centres in bismuth-doped glass [19, 54]. UV laser radiation at 193 nm and 244 nm can also enhance the fluorescence of Bi/Al co-doped optical fibres after H_2 loading, ascribed to the increase of BACs [55, 56]. In addition, laser-induced attenuation change in active optical fibre is another common effect. This change can be photo-bleaching or photo-darkening. Photo-bleaching refers to the decrease of the absorption after the radiation, and photo-darkening is the reverse effect. Photo-darkening is severe in Al-silicate Yb-doped fibres with high Yb^{3+} doping [57]. The

absorption coefficient of Yb^{3+} can be photo-bleached by 977 nm laser radiation [58]. The similar photo-bleaching effect has been observed in thulium-doped fibre [59] as well as BDF [60]. To improve the performance of BDF lasers and amplifiers, the photo-bleaching effect induced by the pump radiation has drawn attention [60]. In this section, the behaviour and mechanism of photo-bleaching of BAC-Si and BAC-Ge in BDF and BEDF have been described in detail.

4.1. Photo-bleaching of BAC-Si

The photo-bleaching of BAC-Si in BEDF under 830 nm pumping has been reported [61]. By pumping the fibre with the power of 0.12 MW/cm^2, the luminescence of BAC-Si at 1420 nm decreases by ~15% after 40 minutes as plotted in **Figure 5(a)**. This decrease of the luminescence is proved to be the bleaching of BAC-Si under the resonant pump radiation. In addition, the self-reversible effect is observed according to the recovery of the absorption of 816 nm, as shown in **Figure 5(b)**. After 2 days at room temperature, both absorption and emission recover to the pristine condition.

Through the investigation of the dependence of bleaching effect upon the pump power, wavelength and temperature, the photo-bleaching mechanism of BAC-Si has further been illuminated [62]. To quantify the bleaching behaviour, the stretched exponential function (SEF) is employed to describe the bleaching process. The SEF is expressed as:

$$I_A(t) = I_{A,\infty}(P) + I_{B,\infty}(P)\, e^{-\left(\frac{t}{\tau(P)}\right)^{\beta(P)}}, \tag{7}$$

where $I_A(t)$ and $I_{A,\infty}$ are the luminescence intensity at time t and at the time when the bleaching effect is saturated under the radiation power P. $I_{B,\infty}$ stands for the bleachable part of the luminescence, τ is the time constant and β is the stretched parameter. Especially, the bleaching ratio is defined as $r_B = \frac{I_{B,\infty}}{I_{A,\infty} + I_{B,\infty}}$. By fitting the decay curve of luminescence of BAC-Si at 1420 nm, it is found that the pump power dependence of r_B and τ shows a high similarity with that of the luminescence intensity as plotted in **Figure 6(a)**, indicating the involvement of the excitation of BAC-Si in the photo-bleaching process. This idea is further proved by the photo-bleaching dependence of BAC-Si on the pump radiation wavelength, as shown in **Figure 6(b)**.

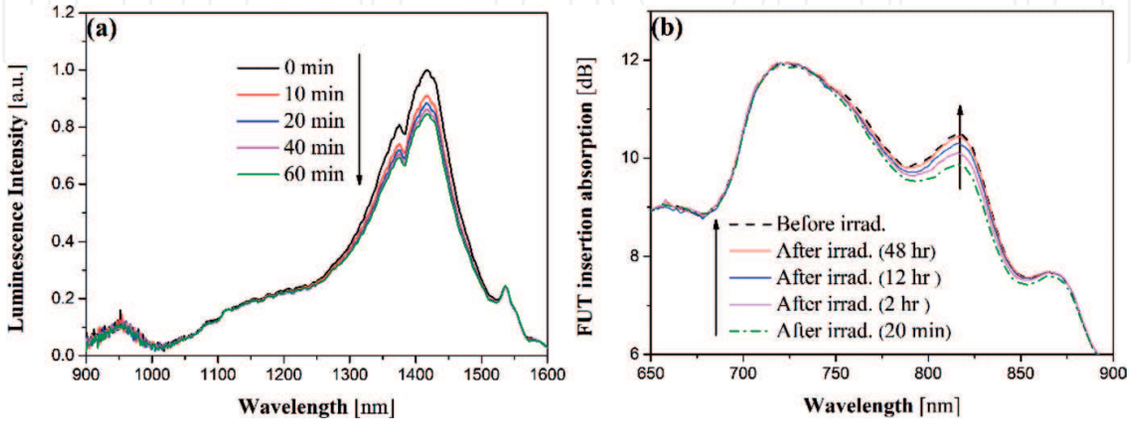

Figure 5. (a) Luminescence spectra of the BEDF under 830 nm pumping measured as a function of time. (b) BEDF insertion absorption spectra obtained before and after irradiation (20 min, 2, 12, and 48 hrs) [61].

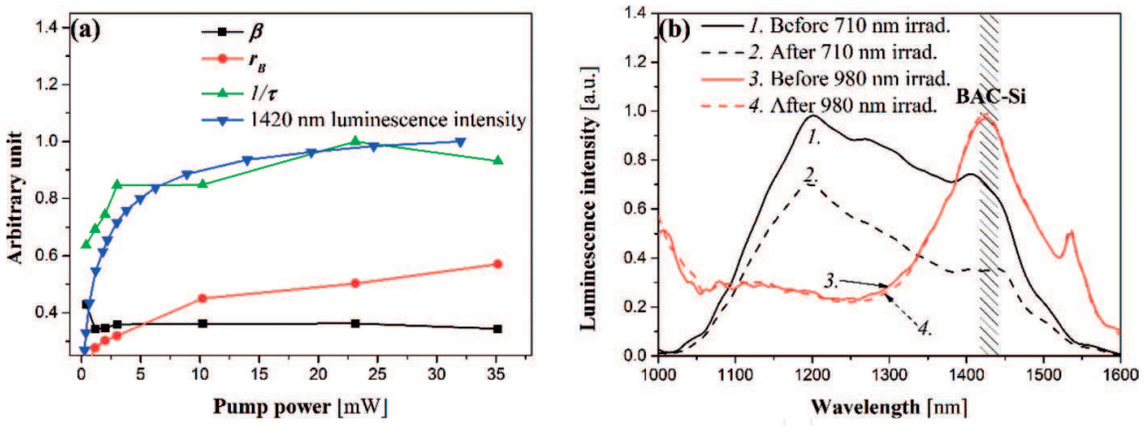

Figure 6. (a) 1420 nm luminescence intensity, the inverse of time constant ($1/\tau$), bleaching ratio (r_B) and stretched parameter (β) vs. pump power. (b) The 710 nm excited luminescence before-*1* and after-*2* 710 nm irradiation and the 830 nm (0.2 mW) excited luminescence before-*3* and after-*4* 980 nm irradiation [62].

In the case of 710 nm irradiation, luminescence of BAC-Si is significantly bleached, while the 830 nm excited luminescence has no change after 30 minutes irradiation of 980 nm pump with 35 mW. The reason for using 830 nm to excite the luminescence is that 980 nm light cannot excite luminescence of BAC-Si. Thereby, it is suggested that the pump laser-induced bleaching effect of BAC-Si is the electron escape from an excited Bi site, expressed as:

$$Bi^{+x}_{BAC-Si} \xrightarrow{h\upsilon} {}^{*}Bi^{+x}_{BAC-Si} \xrightarrow{kT} Bi^{+(x+1)}_{BAC-Si} + e^{-}, \tag{8}$$

where Bi^{+x}_{BAC-Si} is the bismuth ion in BAC-Si with valance state of $+x$, * symbolizes the excited state and kT stands for the thermal energy. First, Bi^{+x}_{BAC-Si} absorbs photon $h\upsilon$ and is excited to the second excited level corresponding to 816 nm. Second, some of ${}^{*}Bi^{+x}_{BAC-Si}$ fall to the lower excited states via non-radiative transition, while some release the electron e^{-} to the acceptor site (a nearby material defect) with the aid of thermal vibrational energy kT and thus induce the decay of luminescence and ground-state absorption. Furthermore, the bleaching ratio of the BAC-Si luminescence can be suppressed by half when lowering the temperature to the liquid nitrogen temperature.

4.2. Photo-bleaching of BAC-Ge

Photo-bleaching of BAC-Ge in BDF has also been observed in bismuth-doped silicate fibre and bismuth-doped germanosilicate fibre [60, 63]. Under the irradiation of 244 nm UV light, the luminescence at 1700 nm of BAC-Ge is totally bleached, as shown in **Figure 7**. Besides, this effect can be activated by 532 nm radiation as well. Further study shows that this photo-bleaching can be reversed by thermal treatment after the irradiation stops and this bleaching-recovery process can be repeated showing a memory effect [64, 65].

It is noted that the structure of BAC-Si/Ge is composed of a Bi ion and SiODC(II)/GeODC(II) [66]. The bleaching of GeODC(II) would deactivate BAC-Ge leading to the decrease of luminescence and absorption when GeODC(II) is photoionized into E′ centre by 244 nm irradiation [67]. So the photo-bleaching of BAC-Ge is caused by the bleaching of the GeODC(II).

http://dx.doi.org/10.5772/intechopen.75106

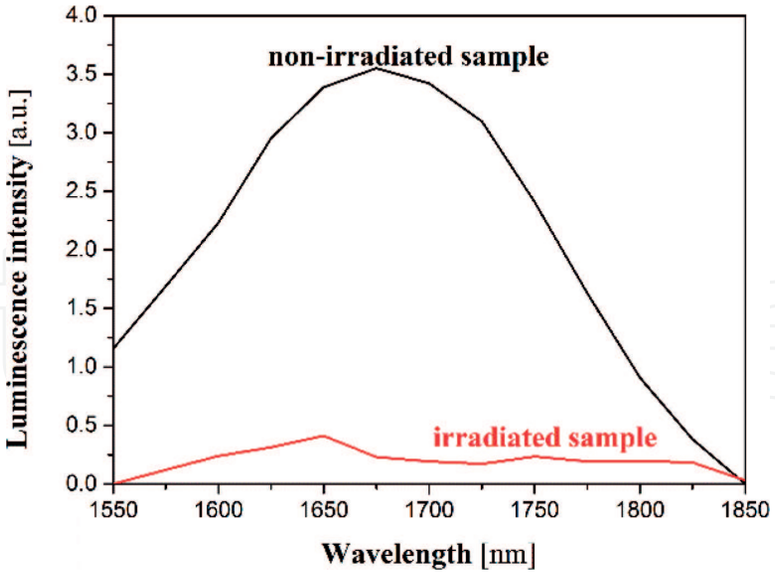

Figure 7. BAC-Ge luminescence spectra at 1700 nm band before and after 1 kJ/cm^2 244 nm irradiation excited at 1460 nm [60, 63].

The destruction of GeODC(II) by UV light leads to the bleaching of BAC-Ge. Such photo-bleaching process can be expressed as [65]:

$$Bi^{+n} + ODC \xrightarrow{h\upsilon} Bi^{+n} + e^{-} + E' \, center \tag{9}$$

which is confirmed by two evidences: 1) the dependence of bleaching speed upon the irradiation power is close to 2 indicating a two-photon process [68]; 2) the thermal dynamic behaviours of BAC-Ge and GeODC are similar [64]. The photo-bleaching effect of BAC-Si in BDF can be explained with a similar mechanism [60]. Therefore, more than one reason possibly induces the photo-bleaching effect dependent upon the material environment.

5. H_2 treatment

Both H_2 and D_2 are the popular reducing agents in the chemical processing of optical fibre. For example, the fabrication of photosensitive optical fibre through H_2 loading, photo-chemical interaction of dissolved H_2 with UV laser-induced electronic excitations significantly quickens grating formation in Ge-doped silica-core fibres. In addition, they can reduce the Bi from the higher valence state to the lower valence state. As a result, H_2 loading will change the absorption and luminescence properties of BDFs. In addition, dissolved H_2 molecules can deactivate excited defects. So, the presence of H_2 molecules leads to the decrease of lifetime and steady-state intensity of triplet luminescence associated with oxygen-deficient centres in fibres, which has been confirmed as one of the key element for the formation of BAC [12]. Hence, in this section, different Bi-doped materials, including crystal, glass and fibre will be treated by H_2 or D_2 under different temperature/pressure. Their spectroscopic properties (e.g., absorption and emission) and photosensitivity before and after H_2 treatment will be described and compared in detail.

5.1. Effect upon spectroscopic properties

5.1.1. Bismuth-doped single crystals annealed in H_2 atmosphere

In Bi: α-BaB_2O_4 crystal, Bi^{3+} will partially substitute Ba^{2+} in the crystal lattice. When the crystal sample is annealed up to 800°C in H_2 atmosphere, a broadband NIR luminescence will appear at 985 nm with FWHM of 187 nm excited at ~808 nm, as shown in **Figure 8** [23]. The lifetime of the emission at 985 nm is about 408 μs. Further investigation of the absorption, excitation and emission spectra indicates that the NIR luminescent centres in the crystal are basically consistent with the multiplets of free Bi^+ for the transition of $^3P_0 \rightarrow {}^1D_2$. Such experimental results demonstrate that thermal annealing of crystal in H_2 atmosphere will produce free electrons in crystal lattice to reduce Bi^{3+} to low-valence Bi^+, accompanied with the creation of O^{2-} vacancies [23].

5.1.2. Bismuth-doped glasses annealed in H_2 atmosphere

However, the heat treatment of bismuth borate glass ($75B_2O_3$–$25Bi_2O_3$) at 450°C under H_2 atmosphere will weaken the luminescence in both the NIR band (1000–1300 nm) and the visible band (650 nm) [69]. The reduction of NIR fluorescence after annealing in oxidation and reduction atmosphere indicates that the valence of the active centres might be a middle state, not the highest Bi^{5+} or the Bi atoms [69]. Similar negative effect of hydrogen annealing of bismuth-doped sodium aluminosilicate glasses at 498°C has been found, which also gives rise to a decrease of the NIR emission and, at the same time, formation of metallic bismuth particles in the surface region. Furthermore, surface tinting as well as the decrease of visible luminescence follow Arrhenius kinetics, suggesting that hydrogen permeation is the rate-governing process [70].

5.1.3. Bismuth-doped fibre after H_2 loading

The presence of H_2 in glass network provides an additional way for non-radiative transitions of activators from excited states to ground states, which therefore negatively affects pump efficiency of fibre lasers and amplifiers. Bi luminescence of hydrogen-impregnated silicate

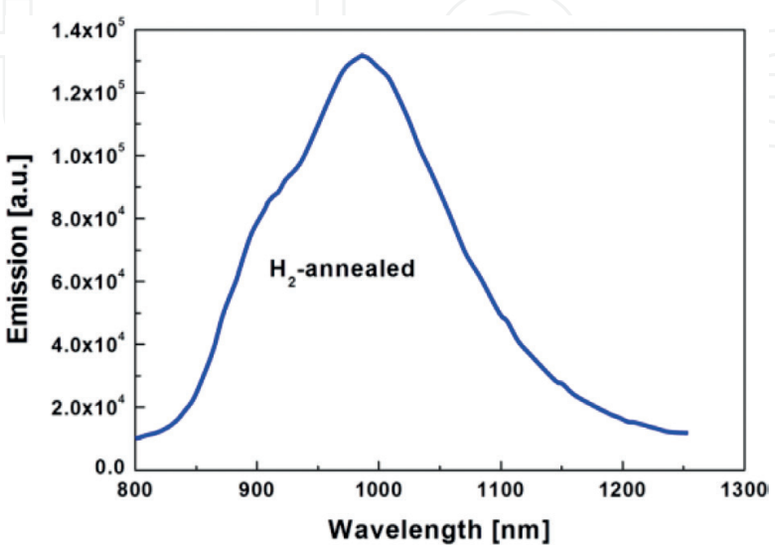

Figure 8. NIR emission spectra of H_2-annealed Bi: α-BaB_2O_4 crystals under excitation at 808 nm [23].

optical fibres will be quenched by deactivation of activators' excited states via collisions with H_2 migrating inside the glass network [71].

In bismuth and fluorine-doped-core silicate fibres, H_2 and D_2 loading at pressures of up to 125 bar leads to a decrease of the steady-state luminescence intensity and lifetime [32]. It is attributed to the appearance of an energy transfer bridge from bismuth clusters to vibrational degrees of freedom of diatomic molecules. In the presence of H_2 or D_2 experiencing random walking in silica, luminescence decay kinetics stops following a single exponential function even in fluorine-free silica-core fibre, especially at higher temperatures. The induced quenching rate increases with the increase of temperature as well and is greater for H_2 molecules than that for D_2. At temperatures below ~250 K, the presence of dissolved molecules has no effect, indicating the primary importance of having rotational degrees of freedom of migrating interstitial diatomic molecules in an excited state for effective quenching of bismuth electronic excitations. Especially, the influence of dissolved D_2 is weaker than that of H_2, due to a greater angular momentum of the D_2 and correspondingly smaller energy of the molecule's rotational quantum. In addition, such experimental results provide additional evidence for a cluster rather than a point defect model for bismuth defects in silica being responsible for NIR luminescence [32].

5.1.4. Bismuth-doped fibre after H_2 loading and thermal annealing

After H_2 loading (100°C, 140 bars, 5 days) and annealing (few seconds at 1000°C) of BDF (SiAlGeP), it is impossible to detect any emission band [72]. Such quenching is due to a similar reason for the degradation of Bi active ions into BiO molecules, Bi metals, and/or Bi_2/Bi_4 clusters. For H_2-loaded BDF, such degradation more probably happens due to the thermochemical reaction between glass network and H_2 molecules, resulting in a partial or complete reduction of the Bi-O linkages. This reaction results in the reduction of Bi ions into Bi metal or Bi atomic clusters and then a complete disappearance of the Bi-related luminescent centres, confirmed by the absence of visible and NIR photoluminescence, as well as the disappearance of all absorption bands in the accessible wavelength range [72].

5.1.5. Bismuth-doped fibre after H_2 loading and UV irradiation

After the irradiation by 193 nm pulsed laser, the H_2-loaded Bi-Al-doped silicate fibre shows huge increase of 1130 and 1390 nm luminescence intensity under 1053 and 1357 nm pumping. This luminescence enhancement seems to be attributed to an increase of the BAC concentration [55], where one evidence is the increase of the absorption peaks of BAC, as shown in **Figure 9**. In addition, the increase of luminescence for H_2-loaded Bi/Al doped optical fibres is also obtained by CW 244 nm laser irradiation. The luminescence increase depends upon accumulated laser fluence [56]. Especially, the luminescence scales with the power of the accumulated dose, where the power exponent m is 0.12 and 0.18 for the CW 244 nm laser and the pulsed 193 nm laser, respectively [56].

5.1.6. Bismuth/erbium co-doped fibre after H_2 loading

Similarly, after H_2 loading (27 hours, 194 bars, 180°C), the absorption of BEDF increases, as shown in **Figure 10(a)**. Meanwhile, the emission is evidently quenched by H_2 loading, as shown in **Figure 10(b)**. The additional appearance of peak at ~1240 nm indicates the diffusion of H_2 molecules in BEDF as in the previous report [32], which is verified by the disappearance of

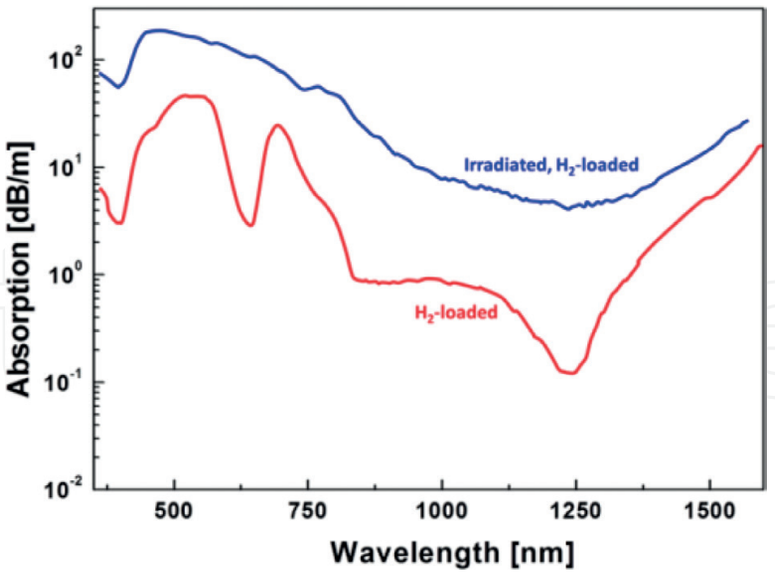

Figure 9. Absorption spectra of H_2-loaded, and irradiated H_2-loaded Bi-Al-doped silicate fibre [55].

the peak after 7 days exposure in air after the loading. The background loss has also increased compared with an unloaded sample. Especially, the emission of BAC-Si at >1380 nm is stronger than that at <1380 nm for the pristine, while after H_2 loading, the emission at >1380 nm becomes weaker than that at <1380 nm. It may due to the increase of the absorption at 1380 nm, which might possibly link with the formation of BAC-Si at 1420 nm [55] or the induced OH absorption at 1380 nm by the reduction of H_2.

5.2. Effect upon photosensitivity

Besides the variation of spectroscopic properties, with H_2 loading (pre-sensitization), the photosensitivity of BDF and BEDF can be changed as well as their stability of the gratings. **Table 2** summarizes the photosensitivity of BDF and BEDF with and without H_2 loading reported so far. The photosensitivity is evidently enhanced by H_2 loading, often leading to higher refractive index changes [73]. The enhanced photosensitivity in H_2-loaded BDF might be attributed

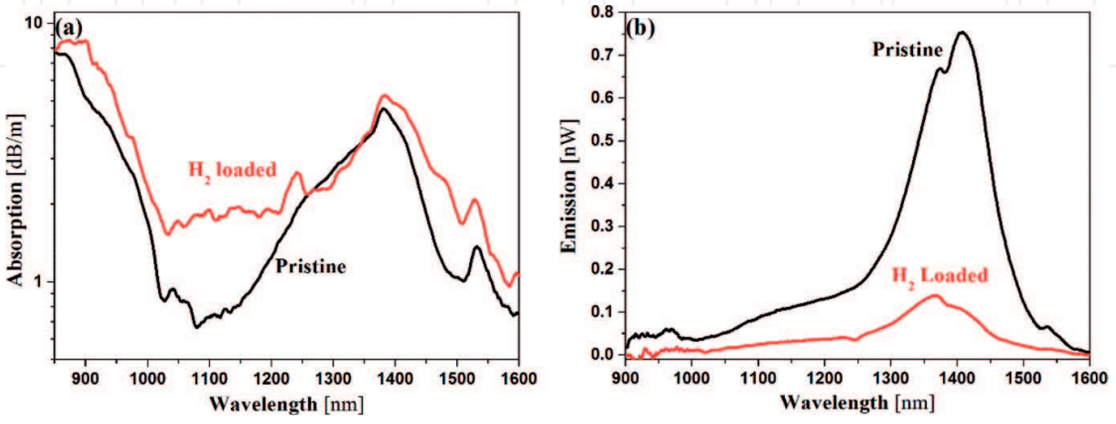

Figure 10. Absorption (a) and emission (b) spectra of BEDF before and after H_2 loaded (27 hours, 194 bars, 180°C) excited by 830 nm.

to Bi-H species (BiH, BiOH, …) [74]. The index changes are sufficient to directly inscribe high-reflective fibre Bragg gratings (FBG) into BDF for laser mirrors. Inscription of FBG directly into the active fibre would reduce the loss caused by splicing and mode field mismatch, leading to higher laser efficiency [74]. Moreover, the thermal stability of these gratings is very important for future applications [75].

5.2.1. Photosensitivity of BDF

The first investigation on the photosensitivity of BDF is performed in 2008 [55]. From fibre grating inscription of the Bi/Al-doped fibre, the induced index change is estimated to be 1×10^{-4} and 1.2×10^{-3} in the H_2 unloaded and H_2-loaded BDFs, respectively [55], showing the enhancement of photosensitivity by H_2 loading. Further investigation demonstrates that a mean index change up to 2.2×10^{-3} can be achieved in H_2-loaded Ge free Bi/Al doped fibre by irradiation of 193 nm pulsed ArF excimer laser, while 2.0×10^{-4} in H_2 unloaded fibres [74, 76]. In addition, the index change greatly depends upon the bismuth dopant concentration, and the higher doping concentration, the higher index change is achieved overall [74, 76]. That is, to say, the high Bi concentration optical fibre exhibits larger index changes for the same amount of irradiation dose [78].

A CW 244 nm Ar^+ laser is also used to fabricate Bragg gratings in pristine and H_2-loaded Bi/Al-doped fibres with index changes as high as 3.6×10^{-4} and 19.3×10^{-4}, respectively [75, 77]. Thermal annealing reveals peaks in the energy distribution at 1.2 and 2.3 eV [75]. Continuous isochronal thermal annealing reveals that although SMF-28e fibres, with and without hydrogen, are more stable than Bi/Al-doped fibres, higher thermal stability for the H_2-loaded Bi/Al-doped fibres is achieved, compared with the pristine one [77]. Moreover, thermal annealing results indicate that the grating in such H_2-loaded BDF has good thermal stability up to 678°C [75].

So far, the maximum index changes as high as $+2.5 \times 10^{-3}$ by 508 W/cm^2 244 nm laser has been achieved in high Bi doping BDF with H_2 loading, giving a maximum reflectivity >93% [78]. In addition, in Bi-doped microstructured optical fibre (BMOF) without H_2 loading, average refractive index changes of 2.7×10^{-4} is induced by a 5.3 kJ/cm^2 193 nm ArF excimer laser [73].

Through the stress study, it is shown in that H_2 loading also leads to a colour centre–based refractive index change. Tensile stress changes indicate a contribution of compaction to the total refractive index change related to volume changes [74, 76]. Especially, the comparison of the measured core stress changes before and after UV irradiation further indicates a compaction contribution to the total refractive index change depends on Bi-concentration [78]. In addition, the irradiation with the higher energy photons for Bi/Al fibre gives rise to a new band that appears at 3.4 eV. This could be an indication that the higher 193 nm photon excites a state that was previously inaccessible with 244 nm photon [82].

5.2.2. Photosensitivity of BEDF

The photosensitivity of BEDF has been studied by Bragg gratings inscription with 193 nm ArF pulsed laser [80] and 244 nm Ar^+ laser [81]. With 193 nm inscription, the average index n_{av} in the Bi-containing fibre with H_2 loading (P = 180 bars, T = 80°C, t = 2 days) grows faster than that in standard highly photosensitive fibre (GF1) and achieves a maximum average index change of 4.5×10^{-4}. Despite the large effective index changes, the index modulation n_{mod} is

Fibre	Key elements	Bi content	H_2 loading	Radiation conditions	Δn	Reference
BDF	Al, Si	0.15–0.3 at%	150 bars for 2 weeks at room temperature	160 mJ/cm^2 193 nm pulsed ArF excimer laser	2.2×10^{-3}	[74, 76]
BDF	Al, Si	0.02 at%	×	500 W/cm^2 CW Ar^+ laser	3.6×10^{-4}	[75]
BDF	Al, Si	0.02 at%	~150 bars for 2 weeks at room temperature	500 W/cm^2 CW Ar^+ laser	1.9×10^{-3}	[77]
BDF	Al, Si	0.15–0.3 at%	~150 bars for 2 weeks at room temperature	508 W/cm^2 CW Ar^+ laser	2.5×10^{-3}	[78]
BDF	Al, Si	0.02 at%	~150 bars for 2 weeks at room temperature	508 W/cm^2 CW Ar^+ laser	1.8×10^{-3}	[78]
BMOF	Si	0.03 at%	×	5.3 kJ/cm^2 193 nm ArF excimer laser	2.7×10^{-4}	[73, 79]
BDF	Al, Si	0.02 at%	×	5.3 kJ/cm^2 193 nm ArF excimer laser	1.0×10^{-4}	[73, 79]
BEDF	Er, Al, P, Ge, Si	0.16 mol% Bi_2O_3	180 bars for 2 days at 80 °C	9.66 J/cm^2 193 nm ArF excimer laser	4.5×10^{-4}	[80]
BEDF	Er, Al, P, Ge, Si	0.16 mol% Bi_2O_3	×	190 mW CW Ar^+ laser	1.1×10^{-4}	[81]

Note: BMPOF-microstructured optical fibre.

Table 2. Summary of photosensitivity in BDFs.

generally found to be quite low in BEDF compared to single-mode germanosilicate fibres. n_{mod} of the grating in pristine fibre decreases rapidly with the increasing temperature. However, the FBG in H_2-loaded BEDF appears more stable when the temperature is under 750°C [80].

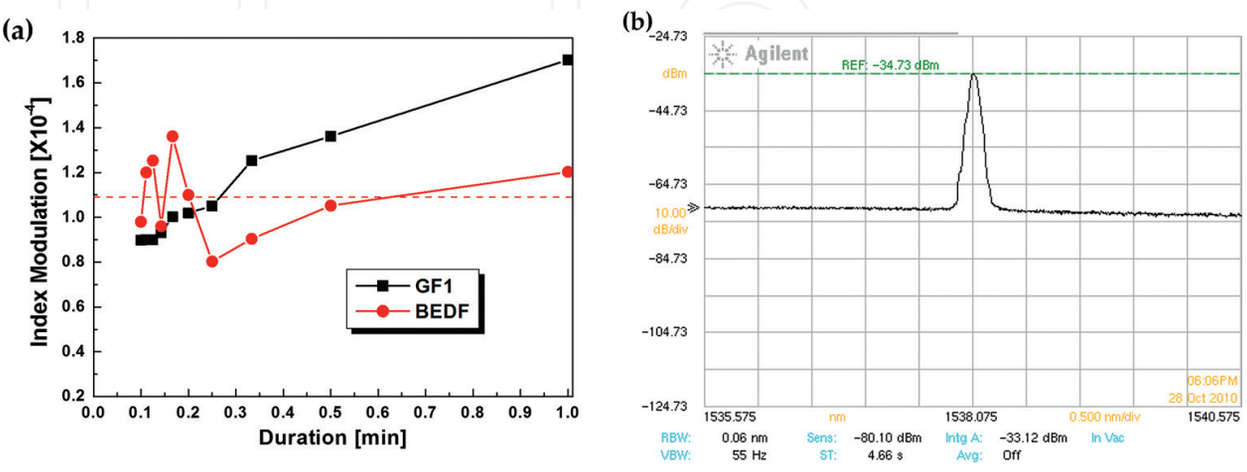

Figure 11. (a) Change in index modulation, n_{mod}, and average index n_{av}, in the BEDF and GF1 fibres vs inscription time with 244 nm laser. (b) Laser spectrum of the DFB fibre laser in 5 nm scanning range. (Fibre length: 20 cm; grating length: 4 cm; pump: 980 nm 70 mW).

Without H_2 loading, BEDF has shown good photosensitivity @ 244 nm [81], comparable to GF1 as expected given similar GeO_2 concentrations, as shown in **Figure 11(a)**. Different from the monotonous increase of GF1 vs the inscription duration, the index modulation of BEDF fluctuates, due to the non-uniformity of the BEDF, with an average index modulation of 1.1×10^{-4}. Especially, based on the phase-shifted gratings fabricated in BEDF, a distributed feedback (DFB) fibre laser operated at ~1538 nm has further been achieved, as shown in **Figure 11(b)**.

6. Summary and outlook

Significant progress has been made in research, development and application of BDF and BEDF since the first demonstration of NIR luminescence in bismuth-doped glass. Many studies have been carried out and demonstrated that the performance, functionality as well as stability, BDF and BEDF of these fibres can be changed by post treatments such as heating, high energy ray radiation, laser exposure and H_2 loading. For example, NIR emission of BAC-Si in BDF excited at 808 nm can be enhanced at high temperature. The thermal treatment could make Bi ions transfer from higher valence to lower valence, even precipitate to Bi_n colloids, which would result in irreversible thermal darkening effect. In addition, the degradation of BAC could occur by implementing thermal treatment in air, while new BAC could form in reduction atmosphere. However, the radiation treatment by gamma ray or electron produces more complicated effects. The radiation can activate the BACs, increase the absorption and enhance the NIR luminescence, dependent upon fibre compositions. Photo-bleaching effect has been observed in both BDF and BEDF by laser radiation. Some photo-bleaching is reversible after undergoing thermal treatment. In addition, the photo-bleaching is found to depend upon radiation wavelength, laser radiation power, temperature as well as material environment. Post treatment by H_2 will not only enhance the photosensitivity of the BDF and BEDF, but also change their spectroscopic properties. As a reducing agent, H_2 will enhance the reduction of Bi from higher valence to lower valence. It could result in the formation of new BAC, but may not increase luminescence due to the deactivation of excited defects or over-reduction. Through the investigations of these post-treatment effects, more understanding of BACs has been obtained and alternative ways to control and regulate the BACs in BDF and BEDF for better performance could be found.

Acknowledgements

Authors are thankful for the support of National Natural Science Foundation of China (61520106014, 61405014 and 61377096), Key Laboratory of In-fibre Integrated Optics, Ministry Education of China, State Key Laboratory of Information Photonics and Optical Communications (Beijing University of Posts and Telecommunications) (IPOC2016ZT07), Key Laboratory of Optical Fibre Sensing and Communications (Education Ministry of China), Key Laboratory of Optoelectronic Devices and Systems of Ministry of Education and Guangdong Province (GD201702) and Science and Technology Commission of Shanghai Municipality, China (SKLSFO2015-01 and 15220721500). The authors also thank Shanghai University for providing them with Fibre Index Profiler for index profiling analysis for the fibre samples.

Author details

Shuen Wei[1], Mingjie Ding[1], Desheng Fan[1], Yanhua Luo[1]*, Jianxiang Wen[2] and Gang-Ding Peng[1]

*Address all correspondence to: yanhua.luo1@unsw.edu.au

1 Photonics and Optical Communications, School of Electrical Engineering and Telecommunications, UNSW Sydney, NSW, Australia

2 Key Laboratory of Specialty Fibre Optics and Optical Access Networks, Shanghai University, Shanghai, China

References

[1] Murata K, Fujimoto Y, Kanabe T, Fujita H, Nakatsuka M. Bi-doped SiO_2 as a new laser material for an intense laser. Fusion Engineering and Design. 1999;**44**(1-4):437-439

[2] Fujimoto Y, Nakatsuka M. Infrared luminescence from bismuth-doped silica glass. Japanese Journal of Applied Physics. 2001;**40**(3B):L279-L281

[3] Ohkura T, Fujimoto Y, Nakatsuka M, Young-Seok S. Local structures of bismuth ion in bismuth-doped silica glasses analyzed using Bi L_{III} X-ray absorption fine structure. Journal of the American Ceramic Society. 2007;**90**(11):3596-3600

[4] Fujimoto Y. New infrared luminescence from Bi-doped glasses. In: Advances in Solid State Lasers Development and Applications. InTech; 2010

[5] Sokolov VO, Plotnichenko VG, Koltashev VV, Dianov EM. Centres of broadband near-IR luminescence in bismuth-doped glasses. Journal of Physics D: Applied Physics. 2009;**42**(9):0954101-0954107

[6] Meng X, Qui J, Peng M, Chen D, Zhao Q, Jiang X, Zhu C. Near infrared broadband emission of bismuth-doped aluminophosphate glass. Optics Express. 2005;**13**(5):1628-1634

[7] Sun H-T, Zhou J, Qiu J. Recent advances in bismuth activated photonic materials. Progress in Materials Science. 2014;**4**:1-72

[8] Dvoyrin VV, Mashinsky M, Dianov EM, Umnikov AA, Yashkov MV, Guranov AN. Absorption, fluorescence and optical amplification in MCVD bismuth-doped silica glass optical fibres. In: 31st European Conference on Optical Communication. 2005. ECOC 2005, Vol. 4; IET. 2005. pp. 949-950

[9] Dianov EM. Amplification in extended transmission bands using bismuth-doped optical fibers. Journal of Lightwave Technology. 2013;**31**(4):681-688

[10] Dianov EM. Bismuth-doped optical fibres: A new breakthrough in near-IR lasing media. Quantum Electronics. 2012;**42**(9):754-761

[11] Riumkin KE, Melkumov MA, Bufetov IA, Shubin AV, Firstov SV, Khopin VF, Guryanov AN, Dianov EM. Superfluorescent 1.44 μm bismuth-doped fiber source. Optics Letters. 2012;**37**(23):4817-4819

[12] Dianov EM. Nature of Bi-related near IR active centers in glasses: State of the art and first reliable results. Laser Physics Letters. 2015;**12**(9):095106 1-6

[13] Dianov EM. Fiber for fiber lasers: Bismuth-doped optical fibers: advances in an active laser media. Laser Focus World. 2015;**51**(9):16

[14] Luo Y, Wen J, Zhang J, Canning J, Peng G-D. Bismuth and erbium codoped optical fiber with ultrabroadband luminescence across O-, E-, S-, C-, and L-bands. Optics Letters. 2012;**37**(16):3447-3449

[15] Sathi ZM, Zhang J, Luo Y, Canning J, Peng G-D. Improving broadband emission within Bi/Er doped silicate fibres with Yb co-doping. Optical Materials Express. 2015;**5**(10):2096-2105

[16] Luo Y, Yan B, Zhang J, Wen J, Peng G-D. Development of Bi/Er co-doped optical fibre (BEDF) for ultra-broadband photonic applications. Frontiers of Optoelectronics. 2017:1-16

[17] Peng G-D, Luo Y, Zhang J, Wen J, Yan B, Canning J. Recent development of new active optical fibres for broadband photonic applications. In: 2013 IEEE 4th International Conference on Photonics (ICP); IEEE. 2013. pp. 5-9

[18] Bufetov IA, Melkumov MA, Firstov SV, Riumkin KE, Shubin AV, Khopin VF, Guryanov AN, Dianov EM. Bi-doped optical fibers and fiber lasers. IEEE Journal of Selected Topics in Quantum Electronics. 2014;**20**(5):111-125

[19] Kononenkoa V, Pashinina V, Galagana B, Sverchkova S, Denkera B, Konova V, Dianov EM. Activation of color centers in bismuth glass by femtosecond laser radiation. Laser Physics. 2011;**21**(9):1585-1592

[20] Sanz O, Haro-Poniatowski E, Gonzalo J, Navarro JF. Influence of the melting conditions of heavy metal oxide glasses containing bismuth oxide on their optical absorption. Journal of Non-Crystalline Solids. 2006;**352**(8):761-768

[21] Khonthon S, Morimoto S, Arai Y, Ohishi Y. Redox equilibrium and NIR luminescence of Bi_2O_3-containing glasses. Optical Materials. 2009;**31**(8):1262-1268

[22] Denker BI, Galagan BI, Musalitin AM, Shulman IL, Sverchkov SE, Dianov EM. Alternative ways to form IR luminescence centers in Bi-doped glass. Laser Physics. 2011;**21**(4):746-749

[23] Xu J, Zhao H, Su L, Yu J, Zhou P, Tang H, Zheng L, Li H. Study on the effect of heat-annealing and irradiation on spectroscopic properties of Bi: α-BaB_2O_4 single crystal. Optics Express. 2010;**18**(4):3385-3391

[24] Dianov EM. Bismuth-doped optical fibers: A challenging active medium for near-IR lasers and optical amplifiers. Light: Science & Applications. 2012;**1**(5):e12 1-7

[25] Xu B, Zhou S, Guan M, Tan D, Teng Y, Zhou J, Ma Z, Hong Z, Qiu J. Unusual luminescence quenching and reviving behavior of Bi-doped germanate glasses. Optics Express. 2011;**19**(23):23436-23443

[26] Peng M, Zollfrank C, Wondraczek L. Origin of broad NIR photoluminescence in bismuthate glass and Bi-doped glasses at room temperature. Journal of Physics: Condensed Matter. 2009;**21**(28):285106 1-6

[27] Peng M, Dong G, Wondraczek L, Zhang L, Zhang N, Qiu J. Discussion on the origin of NIR emission from Bi-doped materials. Journal of Non-Crystalline Solids. 2011;**357**(11):11-13

[28] Hanafusa H, Hibino Y, Yamamoto F. Formation mechanism of drawing-induced E' centers in silica optical fibers. Journal of Applied Physics. 1985;**58**(3):1356-1361

[29] Zlenko AS, Mashinsky VM, Iskhakova LD, Semjonov SL, Koltashev VV, Karatun NM, Dianov EM. Mechanisms of optical losses in Bi:SiO_2 glass fibers. Optics Express. 2012;**20**(21): 23186-23200

[30] Bulatov LI, Mashinsky VM, Dvoirin VV, Kustov EF, Dianov EM, Sukhorukov AP. Structure of absorption and luminescence bands in aluminosilicate optical fibers doped with bismuth. Bulletin of the Russian Academy of Sciences: Physics. 2008;**72**(12):1655-1660

[31] Dvoretskii DA, Bufetov IA, Velmiskin VV, Zlenko AS, Khopin VF, Semjonov VF, Guryanov AN, Denisov LK, Dianov EM. Optical properties of bismuth-doped silica fibres in the temperature range 300-1500 KJ. Journal of Quantum Electronics. 2012;**42**(9):762-769

[32] Bazakutsa AP, Golant KM. Near-infrared luminescence of bismuth in fluorine-doped-core silica fibres. Optics Express. 2015;**23**(3):3818-3830

[33] Bazakutsa AP, Butov OV, Savel'ev EA, Golant KM. Specific features of IR photoluminescence of bismuth-doped silicon dioxide synthesized by plasmachemical method. Journal of Communications Technology and Electronics. 2012;**57**(7):743-750

[34] Granados DR, Kir'yanov AV, Barmenkov YO, Halder A, Das S, Dhar A, Paul MC, Bhadra SK, Didenko SI, Koltashev VV, Plotnichenko VG. Effects of elevating temperature and high-temperature annealing upon state-of-the-art of yttia-alumino-silicate fibers doped with Bismuth. Optical Materials Express. 2016;**6**(2):486-508

[35] Dvoretsky DA, Bufetov IA, Khopin VF, Guryanov AN, Denisov LK, Dianov EM. Optical properties of the bismuth-doped aluminosilicate fiber within the temperature range 300-1500 K. In: Proc. ICONO/LAT; Moscow, Russia. 2013. pp. 18-22

[36] Wei S, Luo Y, Ding M, Cai F, Xiao G, Fan D, Zhao Q, Peng G-D. Thermal effect on attenuation and luminescence of Bi/Er co-doped fiber. IEEE Photonics Technology Letters. 2017;**29**(1): 43-46

[37] Wei S, Luo Y, Ding M, Cai F, Zhao Q, Peng G-D. Annealing effects on bismuth active centers in Bi/Er co-doped fiber. In: 2016 Conference on Lasers and Electro-Optics (CLEO); IEEE. 2016. pp. 1-2

[38] Park SY, Weeks RA, Zuhr RA. Optical absorption by colloidal precipitates in bismuth-implanted fused silica: Annealing behaviour. Journal of Applied Physics. 1995;**77**(12): 6100-6107

[39] Pan Z, Morgan SH, Henderson DO, Park SY, Weeks RA, Magruder RH III, Zuhr RA. Linear and nonlinear optical response of bismuth and antimony implanted fused silica: Annealing effects. Optical Materials. 1995;**4**(6):675-684

[40] Vivona M, Girard S, Marcandella C, Robin T, Cadier B, Cannas M, Boukenter A, Ouerdane Y. Influence of Ce codoping and H_2 pre-loading on Er/Yb-doped fiber: Radiation response characterized by confocal micro-luminescence. Journal of Non-Crystalline Solids. 2011;**357**(8):1963-1965

[41] Girard S, Vivona M, Laurent A, Cadier B, Marcandella C, Robin T, Pinsard E, Boukenter A, Ouerdane Y. Radiation hardening techniques for Er/Yb doped optical fibers and amplifiers for space application. Optics Express. 2012;**20**(8):8457-8465

[42] Sheng Y, Yang L, Luan H, Liu Z, Yu Y, Li J, Dai N. Improvement of radiation resistance by introducing CeO_2 in Yb-doped silicate glasses. Journal of Nuclear Materials. 2012;**427**(1):58-61

[43] Peng T-S, Huang Y-W, Wang LA, Liu R-Y, Chou F-I. Photo-annealing effects on gamma radiation induced attenuation in Erbium doped fibers and the sources using 532-nm and 976-nm lasers. IEEE Transactions on Nuclear Science. 2010;**57**(4):2327-2331

[44] Chang SH, Liu R-Y, Lin C-E, Chou F-I, Tai C-Y, Chen C-C. Photo-annealing effect of gamma-irradiated erbium-doped fibre by femtosecond pulsed laser. Journal of Physics D: Applied Physics. 2013;**46**(49):1-6

[45] Lezius M, Predehl K, Stower W, Turler A, Greiter M, Hoeschen C, Thirolf P, Assmann W, Habs D, Prokofiev A, Ekstrom C, Hansch TW, Holzwarth R. Radiation induced absorption in rare earth doped optical fibers. IEEE Transactions on Nuclear Science. 2012;**59**(2):425-433

[46] Fox BP, Simmons-Potter K, Moore SW, Fisher JH, Meister DC. Gamma-radiation-induced photodarkening in actively pumped Yb^{3+}-doped optical fiber and investigation of post-irradiation transmittance recovery. No. SAND2009-4532C. Albuquerque, NM (United States): Sandia National Laboratories (SNL-NM); 2009

[47] Wen J, Liu W, Dong Y, Luo Y, Peng GD, Chen N, Pang F, Chen Z, Wang T. Radiation-induced photoluminescence enhancement of Bi/Al-codoped silica optical fibers via atomic layer deposition. Optics Express. 2015;**23**(22):29004-29013

[48] Yan B, Luo Y, Sporea D, Mihai L, Negut D, Ding M, Wang C, Wen J, Sang X, Peng G-D. Enhanced gamma radiation effect in Bi/Er co-doped optical fibre by co-doping Yb. Asia Communications and Photonics Conference. Optical Society of America. 2016: AF2A, p. 135

[49] Yan B, Luo Y, Sporea D, Mihai L, Negut D, Sang X, Wen J, Xiao G, Peng G-D. Gamma radiation-induced formation of bismuth related active centre in Bi/Er/Yb co-doped fibre. Asia Communications and Photonics Conference. Optical Society of America; 2015: ASu2A-56

[50] Sporea D, Mihai L, Negut D, Luo Y, Yan B, Ding M, Wei S, Peng G-D. γ irradiation induced effects on bismuth active centres and related photoluminescence properties of Bi/Er co-doped optical fibres. Scientific Reports. 2016;**6**:29827 1-11

[51] Firstov SV, Khopin VF, Alyshev SV, Firstova EG, Riumkin KE, Melkumov MA, Khegai AM, Kashaykin PF, Guryanov AN, Dianov EM. Effect of gamma-irradiation on the optical properties of bismuth-doped germanosilicate fibers. Optical Materials Express. 2016;**6**(10):3303-3308

[52] Kir'yanov AV, Dvoyrin AV, Mashinsky VM, Il'ichev NN, Kozlova NS, Dianov EM. Influence of electron irradiation on optical properties of bismuth doped silica fibers. Optics Express. 2011;**19**(7):6599-6608

[53] Kir'yanov AV. Effects of electron irradiation upon absorptive and fluorescent properties of some doped optical fibers. In: Radiation Effects in Materials. InTech; 2016

[54] Peng M, Zhao Q, Qiu J, Wondraczek L. Generation of emission centers for broadband NIR luminescence in bismuthate glass by femtosecond laser irradiation. Journal of the American Ceramic Society. 2009;**92**(2):542-544

[55] Ban C, Bulatov LI, Dvoyrin VV, Mashinsky VM, Limberger HG, Dianov EM. Infrared luminescence enhancement by UV-irradiation of H_2-loaded Bi-Al-doped fiber. In: 35th European Conference on Optical Communication, 2009. ECOC'09. IEEE. 2009. pp. 1-2

[56] Violakis G, Limberger HG, Mashinsky VM, Dianov EM. Dose dependence of luminescence increase in H_2-loaded Bi-Al co-doped optical fibers by cw 244-nm and pulsed 193-nm laser irradiation. Optical Fiber Communication Conference. Optical Society of America; 2013. OTh4C-2

[57] Piccoli R, Robin T, Brand T, Klotzbach U, Taccheo S. Effective photodarkening suppression in Yb-doped fiber lasers by visible light injection. Optics Express. 2014;**22**(7):7638-7643

[58] Guzman Chávez AD, Kir'yanov AV, Barmenkov YO, Il'ichev NN. Reversible photodarkening and resonant photobleaching of ytterbium-doped silica fiber at in-core 977-nm and 543-nm irradiation. Applied Physics Letters. 2007;**4**(10):734-739

[59] Laperle P, Chandonnet A, Vallée R. Photobleaching of thulium-doped ZBLAN fibers with visible light. Optics Letters. 1997;**22**(3):178-180

[60] Firstov S, Alyshev S, Melkumov M, Riumkin K, Shubin A, Dianov EM. Bismuth-doped optical fibers and fiber lasers for a spectral region of 1600-1800 nm. Optics Letters. 2014;**39**(24):6927-6930

[61] Ding M, Wei S, Luo Y, Peng G-D. Reversible photo-bleaching effect in a bismuth/erbium co-doped optical fiber under 830 nm irradiation. Optics Letters. 2016;**41**(20):4688-4691

[62] Ding M, Fang J, Luo Y, Wang W, Peng G-D. Photo-bleaching mechanism of the BAC-Si in bismuth/erbium co-doped optical fibers. Optics Letters. 2017;**42**(24):5222-5225

[63] Firstov S, Alyshev S, Khopin V, Melkumov M, Guryanov A, Dianov EM. Photobleaching effect in bismuth-doped germanosilicate fibers. Optics Express. 2015;**23**(15):19226-19233

[64] Firstov SV, Firstova EG, Alyshev SV, Khopin VF, Riumkin KE, Melkumov MA, Guryanov AN, Dianov EM. Recovery of IR luminescence in photobleached bismuth-doped fibers by thermal annealing. Laser Physics. 2016;**26**(8):084007

[65] Firstov SV, Alyshev SV, Kharakhordin AV, Riumkin KE, Dianov EM. Laser-induced bleaching and thermo-stimulated recovery of luminescent centers in bismuth-doped optical fibers. Optical Materials Express. 2017;**7**(9):3422-3432

[66] Dianov EM. On the nature of near-IR emitting Bi centres in glass. Journal of Quantum Electronics. 2010;**40**(4):283

[67] Skuja L. Optically active oxygen-deficiency-related centers in amorphous silicon dioxide. Journal of Non-Crystalline Solids. 1998;**239**(1):16-48

[68] Firstov SV, Alyshev SV, Firstova EG, Melkumov MA, Khegay AM, Khopin VF, Guryanov AN, Dianov EM. Dependence of the photobleaching on laser radiation wavelength in bismuth-doped germanosilicate fibers. Journal of Luminescence. 2017;**182**:87-90

[69] Qiu YQ, Kang J, Li CX, Dong XY, Zhao C-L. Broadband near-infrared luminescence in bismuth borate glasses. Laser Physics. 2010;**20**(2):487-492

[70] Nielsen KH, Smedskjaer MM, Peng M, Yue Y, Wondraczek L. Surface-luminescence from thermally reduced bismuth-doped sodium aluminosilicate glasses. Journal of Non-Crystalline Solids. 2012;**358**(23):3193-3199

[71] Bazakutsa AP, Butov OV, Golant KM. Influence of hydrogen loading on active fibers. Optical Fiber Communication Conference and Exposition and the National Fiber Optic Engineers Conference (OFC/NFOEC); IEEE. 2013. pp. 1-3

[72] Truong VG, Bigot L, Lerouge A, Douay M, Razdobreev I. Study of thermal stability and luminescence quenching properties of bismuth-doped silicate glasses for fiber laser applications. Applied Physics Letters. 2008;**92**(4):1-3

[73] Violakis G, Limberger HG, Zlenko AS, Semjonov SL, Bufetov IA, Mashinsky VM, Vel'miskin VV, Dianov EM. Fabrication of Bragg gratings in microstructured and step index Bi-SiO_2 optical fibers using an ArF laser. Optics Express. 2012;**20**(26):B118-B123

[74] Ban C, Limberger HG, Mashinsky V, Dvoyrin V, Dianov EM. UV-Photosensitivity of Germanium-Free Bi-Al Silica Fibers. Bragg Gratings, Photosensitivity, and Poling in Glass Waveguides. Optical Society of America. Karlsruhe, Germany. 2010. BWD3

[75] Violakis G, Limberger HG, Mashinsky V, Dianov EM. Fabrication and thermal decay of fiber Bragg gratings in Bi-Al co-doped optical fibers. In: 2011 37th European Conference and Exhibition on Optical Communication (ECOC). IEEE; 2011. pp. 1-4

[76] Ban C, Limberger HG, Mashinsky V, Dianov EM. Photosensitivity and stress changes of Ge-free Bi-Al doped silica optical fibers under ArF excimer laser irradiation. Optics Express. 2011;**19**(27):26859-26865

[77] Violakis G, Limberger HG, Mashinsky VM, Dianov EM. Fabrication and thermal decay of fiber Bragg gratings in pristine and H_2-loaded Bi-Al co-doped optical fibers. Optics Express. 2011;**19**(26):B350-B356

[78] Violakis G, Limberger HG, Mashinsky V, Dianov EM. Strong fiber Bragg gratings in Bi-Al co-doped H_2-loaded optical fibers using CW-Ar^+ laser. Optical Fiber Communication Conference and Exposition (OFC/NFOEC), 2011 and the National Fiber Optic Engineers Conference; IEEE. 2011. pp. 1-3

[79] Violakis G, Limberger HG, Zlenko AS, Semjonov SL, Mashinsky VM, Dianov EM. Fabrication of Bragg gratings in microstructured Bi: SiO_2 optical fiber using an ArF laser. European Conference and Exhibition on Optical Communication. Optical Society of America; 2012. We. 1. F. 3

[80] Cook K, Shao L-Y, Canning J, Wang T, Luo Y, Peng G-D. Bragg gratings in few-mode Er/Al/Bi/P Co-doped germanosilicate ring-core fibre. OFS2012 22nd International Conference on Optical Fiber Sensors, Vol. 8421. International Society for Optics and Photonics; 2012. 842155 1-4

[81] Qi H, Luo Y, Yang H, Zhang J, Canning J, Peng G-D. Photosensitivity, phase shifted grating and DFB fibre laser in bismuth/erbium co-doped germanosilicate optical fibre. 19th Optoelectronics and Communications Conference (OECC) and the 39th Australian Conference on Optical Fibre Technology (ACOFT); Engineers Australia. 2014. pp. 495-497

[82] Violakis G, Saffari P, Limberger HG, Mashinsky VM, Dianov EM. Thermal decay of UV Ar+ and ArF excimer laser fabricated Bragg gratings in SMF-28e and Bi-Al-doped optical fiber. Bragg Gratings, Photosensitivity, and Poling in Glass Waveguides. Optical Society of America; 2012. BM4D-6

IntechOpen